

1  
2  
3  
4 1  **$\delta^{18}\text{O}$  and  $\delta^{13}\text{C}$  of *Cyprideis torosa* from coastal lakes: modern systematics and down-**  
5 **core interpretation**

6 2 Roberts, L.R.<sup>1,2,a</sup>, Holmes, J.A.<sup>2\*</sup>, Sloane, H.J.<sup>3</sup>, Arrowsmith, C.<sup>3</sup>, Leng, M.J.<sup>3,4</sup> and Horne, D.J.<sup>1</sup>  
7  
8 4

9 5 <sup>1</sup>*School of Geography, Queen Mary University of London, Mile End Road, London, E1 4NS,*  
10 *UK*  
11 6

12 7 <sup>2</sup>*Environmental Change Research Centre, Department of Geography, University College*  
13 *London, Gower Street, London, WC1E 6BT, UK*  
14 8

15 9 <sup>3</sup>*National Environmental Isotope Facility, British Geological Survey, Keyworth, Nottingham,*  
16 *NG12 5GG, UK*  
17 10

18 11 <sup>4</sup>*Centre for Environmental Geochemistry, School of Biosciences, University of Nottingham,*  
19 *Sutton Bonington Campus, Loughborough LE12 5RD, UK*  
20 12

21 13  
22 14 <sup>a</sup>*Current address: Centre for Environmental Geochemistry, School of Geography, University*  
23 *of Nottingham, Nottingham, NG7 2RD, UK*  
24 15

25 16  
26 17 [\\*j.holmes@ucl.ac.uk](mailto:*j.holmes@ucl.ac.uk)  
27 18

28 19  
29 20 **Abstract**  
30 21

31 22 Stable isotope analyses of ostracod shells are a commonly-used proxy for  
32 23 palaeoenvironmental reconstruction. Although the fundamental controls on isotope  
33 24 composition of ostracod shells are well understood and, in some instances, quantifiable, the  
34 25 paleoclimatic and palaeoenvironmental interpretation of records from lake sediments depends  
35 26 strongly on the characteristics of individual lakes including the climatic setting, depth, volume,  
36 27 hydrology, aquatic vegetation and catchment properties. This is particularly important for  
37 28 coastal lakes where physio-chemical variations may occur on diurnal timescales. Here, we  
38 29 combine variations in  $\delta^{18}\text{O}_{\text{water}}$ ,  $\delta^{18}\text{O}_{\text{ostracod}}$  and  $\delta^{13}\text{C}_{\text{ostracod}}$ , hourly water temperature, and  
39 30  $\text{Mg}/\text{Ca}_{\text{ostracod}}$  inferred water temperatures (constraining calcification temperature) to improve  
40 31 palaeoenvironmental interpretation and provide insights into lake carbon cycle. The dataset  
41 32 improves understanding of complex coastal lake site systematics and downcore interpretation  
42 33 of stable isotopes from *C. torosa*, a geographically widespread brackish water ostracod. The  
43 34  $\delta^{18}\text{O}_{\text{ostracod}}$  values show a complex relationship with temperature and suggest, in most  
44 35 circumstances, that  $\delta^{18}\text{O}_{\text{water}}$  is the dominant control on  $\delta^{18}\text{O}_{\text{ostracod}}$ . During times of fresher  
45 36 water,  $\delta^{13}\text{C}_{\text{ostracod}}$  increases, suggesting increasing aquatic productivity. Above a certain  
46 37  $\delta^{18}\text{O}_{\text{water}}$  threshold however, aquatic productivity begins to decline. The interpretation of  
47 38  $\delta^{13}\text{C}_{\text{ostracod}}$  in some coastal lakes, may therefore be dependent on understanding of the range  
48 39 of expected  $\delta^{18}\text{O}_{\text{water}}$ . Due to short-term (diurnal to seasonal) variations that cause large  
49  
50  
51  
52  
53  
54  
55  
56  
57  
58  
59  
60

61  
62  
63 40 ranges in  $\delta^{18}\text{O}_{\text{water}}$  and  $\delta^{18}\text{O}_{\text{ostracod}}$ , stable isotope analyses of *C. torosa* should be: 1)  
64 41 undertaken on multiple single shells 2) where carapaces are preserved, paired with trace-  
65 42 element/Ca analyses on the same individual; and 3) undertaken alongside a study of the  
66 43 modern lake system.  
67  
68  
69  
70

71 45 **Keywords:** *Cyprideis torosa*; ostracods; stable isotopes; oxygen isotope; carbon isotope;  
72 46 coastal lakes; palaeoenvironmental reconstruction  
73

## 74 47 75 48 76 49 **1. Introduction**

77 50 Inorganic and biogenic carbonates precipitated from lake water provide an archive of past  
78 51 oxygen ( $\delta^{18}\text{O}$ ) and carbon ( $\delta^{13}\text{C}$ ) isotope composition of host water and dissolved inorganic  
79 52 carbon (DIC), and, for oxygen, potentially water temperature as well. For palaeoenvironmental  
80 53 studies, there are advantages in analysing biogenic over endogenic carbonate. For example,  
81 54 the use of biogenic carbonate can reflect taphonomic or habitat-specific stable isotope  
82 55 composition while the use of endogenic carbonate does not guarantee that the material was  
83 56 formed in water and may include a detrital component. The calcite shells of ostracods (small  
84 57 bivalved crustaceans) are often abundant and well preserved in sediments, providing a  
85 58 commonly used proxy for palaeoenvironmental studies. The calcification of carapaces occurs  
86 59 within hours to a few days with no subsequent addition of calcite, thus providing a 'snapshot'  
87 60 of water conditions at the timing of calcification. This is very different to the 'averaging' of  
88 61 conditions recorded by endogenic carbonate and other types of biogenic carbonates that  
89 62 accumulate incrementally. Where the life cycle and habitat preferences of a species is known,  
90 63 isotopic records may therefore reflect seasonal and habitat-specific information (e.g. von  
91 64 Grafenstein *et al.*, 1999a).  
92  
93  
94  
95  
96  
97  
98  
99

100 65 The oxygen-isotope composition of biogenic and endogenic calcite is determined by water  
101 66 temperature and water-isotope composition, along with any kinetic vital effects. During growth,  
102 67 the carbonate ions ( $\text{CO}_3^{2-}$ ) are generally thought to be in equilibrium with the isotope  
103 68 composition of the water. However, since  $\text{CO}_3^{2-}$  ions are precipitated together with calcium to  
104 69 form calcium carbonate, heavy isotopes are preferentially incorporated (Kim and O'Neil, 1997;  
105 70 Romanek *et al.*, 1992). Substantial evidence exists to suggest that ostracod calcite is  
106 71 precipitated out of oxygen isotope equilibrium with the host water, by +3 ‰ or more (Xia *et al.*,  
107 72 1997; von Grafenstein *et al.*, 1999b; Chivas *et al.*, 2002; Keatings *et al.*, 2002; Decrouy *et al.*,  
108 73 2011). The magnitude of offset appears to vary taxonomically; vital offsets are similar for  
109 74 members of the same genus, or even subfamily.  
110  
111  
112  
113  
114  
115  
116  
117  
118  
119  
120

121  
122  
123 76 Since the  $\delta^{18}\text{O}_{\text{calcite}}$  is a function of temperature and  $\delta^{18}\text{O}_{\text{water}}$ , if the calcification temperature  
124 77 is known independently, the  $\delta^{18}\text{O}_{\text{water}}$  can be calculated, for example using the equation of Kim  
125 78 and O'Neil (1997),  $1000\ln\alpha_{(\text{calcite-water})} = 18.03(10^3 T^{-1}) - 32.42$ . However, the equation relies on  
126 79 the assumption that mineral precipitation is controlled by  $\delta^{18}\text{O}_{\text{water}}$  at the time of calcification  
127 80 and that any vital effects are known and accounted for (von Grafenstein *et al.*, 1999b).  
128 81  $\delta^{18}\text{O}_{\text{water}}$  is a function of  $\delta^{18}\text{O}$  rainfall,  $\delta^{18}\text{O}$  of catchment inputs, evaporative enrichment or a  
129 82 combination of all three.  $\delta^{18}\text{O}_{\text{ostracod}}$  has, therefore, been used to reconstruct: the composition  
130 83 of rainfall (von Grafenstein, 2002), effective moisture (Hodell *et al.*, 1991; Street-Perrott *et al.*,  
131 84 2000; Holmes *et al.*, 2010), meltwater influx (Dettman *et al.*, 1995), and changes in seawater  
132 85 input (Janz and Vennemann, 2005; Williams *et al.*, 2006).  
133  
134  
135  
136  
137  
138

139 86  
140 87 The  $\delta^{13}\text{C}$  of ostracod shells is primarily determined by the  $\delta^{13}\text{C}$  of DIC with only a small  
141 88 temperature effect during calcite precipitation (Leng and Marshall, 2004). Offsets from carbon-  
142 89 isotope equilibrium appear to be negligible although, at present, there is limited understanding  
143 90 of carbon isotope fractionation in ostracod shells. Since many ostracod species are not  
144 91 nektonic (including *Cyprideis torosa*), the  $\delta^{13}\text{C}$  often does not reflect open water conditions,  
145 92 but more localised dissolved inorganic carbon (DIC) of pore water or water at the sediment  
146 93 interface, which is often more strongly correlated with the breakdown of sediment organic  
147 94 matter than primarily productivity. However, in very shallow well-mixed waterbodies with few  
148 95 submerged macrophytes, there may be little difference in DIC composition between the  
149 96 ambient water in the water column and the sediment-water interface. Furthermore, it is still  
150 97 unknown if ostracod species calcify in the sediment or in the water column. Despite this,  
151 98 Wrozyzna *et al.* (2012) showed that with increasing productivity, plankton preferentially uptake  
152 99  $^{12}\text{C}$  and the remaining DIC is enriched with  $^{13}\text{C}$ , which is consequently incorporated into  
153 100 carbonates. As a result of decay of organic matter, ambient water is enriched in  $^{12}\text{C}$  and  
154 101 ostracods are consequently depleted in  $^{13}\text{C}$  so that  $\delta^{13}\text{C}$  values are more negative. Differences  
155 102 in species  $\delta^{13}\text{C}$  values are therefore often regarded as habitat effects rather than true vital  
156 103 effects (Heaton *et al.* 1995). Given this, ostracod-based  $\delta^{13}\text{C}$  are not straight forward to  
157 104 interpret, but they have been used to reconstruct aquatic productivity (Anadón *et al.*, 2006; Li  
158 105 and Liu, 2014) and provide evidence for methane formation (Bridgwater *et al.*, 1999).  
159  
160  
161  
162  
163  
164  
165  
166  
167

168 106  
169 107 Although the fundamental controls on isotope composition of ostracod shells are well  
170 108 understood and, in some instances, quantifiable, the paleoclimatic and palaeoenvironmental  
171 109 interpretation of isotope records from lake sediments depends strongly on the characteristics  
172 110 of individual lakes including the climatic setting, depth, volume, hydrology, aquatic vegetation  
173 111 and catchment properties. These are particularly important considerations for coastal lakes,  
174 112 ponds, and lagoons where complex diurnal mixing of water masses often results in changes  
175  
176  
177  
178  
179  
180

181  
182  
183  
184  
185  
186  
187  
188  
189  
190  
191  
192  
193  
194  
195  
196  
197  
198  
199  
200  
201  
202  
203  
204  
205  
206  
207  
208  
209  
210  
211  
212  
213  
214  
215  
216  
217  
218  
219  
220  
221  
222  
223  
224  
225  
226  
227  
228  
229  
230  
231  
232  
233  
234  
235  
236  
237  
238  
239  
240

113 to solute chemistry, water depth, and, in some cases, temperature. Marginal-marine  
114 environments including estuaries, deltas and coastal lakes/ponds with both direct and indirect  
115 seawater connection are complex, unstable, and often unpredictable environments due to the  
116 variation in physio-chemical conditions from the complex mixing of fresh- and sea- water.  
117 These variations are due to climatic (precipitation/evaporation cycles) and dynamic (tides,  
118 currents, freshwater drainage and sea level changes) factors (Carbonel, 1988; Dix *et al.*,  
119 1999). The mixing of freshwater and seawater results in a theoretical straight mixing line of  
120  $\delta^{18}\text{O}$ . However, Anadón *et al.* (2002) suggest that the natural variations in this relationship,  
121 often resulting from a third end member such as groundwater, prohibits the use of  $\delta^{18}\text{O}_{\text{ostracod}}$   
122 as a palaeotemperature proxy unless paired with Mg/Ca-inferred temperatures (e.g. Ingram  
123 *et al.* 1998). An understanding of the modern isotope systematics of the site, and the life-cycle  
124 and habitat preferences of the target ostracod species are therefore important constraints  
125 when interpreting isotopic signatures (Decrouy *et al.*, 2011).

126  
127 The robust well-calcified carapace of *Cyprideis torosa* is a valuable source of Quaternary  
128 paleoclimatic information. It is geographically widespread (Wouters, 2017) and tolerant of a  
129 wide range of ecological conditions. Most notably, it is extremely euryhaline, and found in  
130 waters from fresh to hypersaline (De Deckker and Lord, 2017; Pint and Frenzel, 2017; Scharf  
131 *et al.*, 2017) although in saline waters it is restricted to those with a marine-like chemistry.  
132 Furthermore there is a good understanding of the adult life-cycle (e.g. Heip, 1976) and there  
133 are existing Mg/Ca palaeotemperature calibrations (e.g. Wansard 1996; De Deckker *et al.*  
134 1999).

135  
136 Due to temperature and  $\delta^{18}\text{O}_{\text{water}}$  varying on short (diurnal) timescales in coastal lakes, water  
137 conditions at the time of ostracod sample collection can be substantially different to those at  
138 the time of shell calcification. As such, establishing the temperature and  $\delta^{18}\text{O}_{\text{water}}$  at the exact  
139 time of shell calcification for *C. torosa* is difficult (Marco-Barba *et al.*, 2012; Bodergat *et al.*  
140 2014). There are therefore two large uncertainties when interpreting *C. torosa* stable isotope  
141 records from coastal lakes; 1) what the dominant controls are on  $\delta^{18}\text{O}_{\text{ostracod}}$ , and 2) whether  
142 short-term (seasonal) lake variations are recorded in sediment records. There are often large  
143 uncertainties in the interpretation of stable isotope signals from *C. torosa*, in part arising from  
144 the paucity of studies into the impact of the diurnal and seasonal variations in coastal lakes  
145 on the isotope geochemistry of ostracod shells. Here, we investigate how the isotope  
146 systematics of a coastal pond are recorded in shells of *C. torosa* using a dataset of water  
147 isotopes, water chemistry and ostracod isotopes in order to improve the interpretation of  
148 ostracod stable isotope signals from sediment records. We combine measurements of  
149  $\delta^{18}\text{O}_{\text{ostracod}}$  with Mg/Ca<sub>ostracod</sub>-inferred water temperatures to back calculate  $\delta^{18}\text{O}_{\text{water}}$ , and



241  
242  
243  
244  
245  
246  
247  
248  
249  
250  
251  
252  
253  
254  
255  
256  
257  
258  
259  
260  
261  
262  
263  
264  
265  
266  
267  
268  
269  
270  
271  
272  
273  
274  
275  
276  
277  
278  
279  
280  
281  
282  
283  
284  
285  
286  
287  
288  
289  
290  
291  
292  
293  
294  
295  
296  
297  
298  
299  
300

150 evaluate these using measurements of seasonal and diurnal water temperature and of water-  
151 isotope composition. A more limited set of carbon-isotope data is used to investigate seasonal  
152 changes in carbon-cycling within the lake. Understanding the nature of these variations and  
153 their controls has important implications for the interpretation of fossil records from similar  
154 environments. The results presented here follow a previous study using the  $Mg/Ca_{ostracod}$  of  
155 the same specimens to track the seasonal calcification of individuals within a population  
156 (Roberts *et al.*, 2020).

157

## 158 **2. Methods**

159

### 160 **2.1 Field methods**

161

162 Material for this study collected from a shallow (< 1 m) coastal pond free from submerged and  
163 floating macrophytes in Pegwell Bay Nature Reserve, Kent, SE UK (Fig. 1), where *C. torosa*  
164 is particularly abundant, in August and December 2016 and April, June and September 2017.  
165 Ostracods were collected in a 250  $\mu$ m zooplankton net from the top 1 cm of sediment at  
166 location 'X' (Fig. 1). Adult carapaces with soft tissue and appendages (indicating that the  
167 individuals were alive at the time of collection) were selected for geochemical analyses. Water  
168 samples for oxygen and hydrogen isotope composition were collected as spot samples for all  
169 dates except June 2017 when samples were collected hourly from low to high tide to capture  
170 diurnal hydro-chemical variability. A seawater end-member sample was collected adjacent to  
171 Ramsgate Harbour in April 2017. In situ measurements of conductivity and temperature were  
172 taken using a YSI 30 handheld probe calibrated and recorded at 25 °C. Hourly subsurface (~  
173 10cm) water temperature was recorded from August 2016 to September 2017 using a Tinytag  
174 Aquatic 2 temperature logger with temperature range -40 °C to +70 °C. For the April and June  
175 2017 sampling, in situ alkalinity as  $CaCO_3$  equivalent was determined using a Hach Digital  
176 Titrator, 1.6N Sulphuric acid ( $H_2SO_4$ ) cartridge and Phenolphthalein and Bromcresol Green-  
177 Methyl Red indicators.

178

### 179 **2.2 Laboratory methods**

180

181 Stable isotope analysis was undertaken on single left valves using an IsoPrime dual inlet mass  
182 spectrometer plus Multiprep at the British Geological Survey. Isotope values ( $\delta^{13}C$ ,  $\delta^{18}O$ ) are  
183 reported as per mille (‰) deviations of the isotope ratios ( $^{13}C/^{12}C$ ,  $^{18}O/^{16}O$ ) calculated to the  
184 VPDB scale using a within-run laboratory standard calibrated against NBS-19. The Craig  
185 correction was applied to account for  $^{17}O$ . Analysis of the in-house standard calcite (KCM)

301  
302  
303 186 gave good reproducibility of  $\pm 0.04$  for both  $\delta^{13}\text{C}$  and  $\delta^{18}\text{O}$  over 72 determinations. Mg/Ca and  
304 187 Sr/Ca determinations were undertaken on the corresponding right valves of the same  
305 188 individuals used for stable isotope analyses, as described in Roberts *et al.* (2020).  
306  
307  
308

309 190  $\delta^{18}\text{O}$  analyses of water were undertaken using the  $\text{CO}_2$  equilibration method on an IsoPrime  
310 191 100 mass spectrometer plus Aquaprep at the British Geological Survey. Hydrogen isotope  
311 192 ( $\delta^2\text{H}$ ) measurements of water were made using an online Cr reduction method with a  
312 193 EuroPyrOH-3110 system coupled to a IsoPrime mass spectrometer. Values are reported as  
313 194 per mille (‰) deviations of the isotope ratios ( $^{18}\text{O}/^{16}\text{O}$  and  $^2\text{H}/^1\text{H}$ ) calculated to the VSMOW  
314 195 scale. Internal quality control standards are calibrated against the international standards  
315 196 VSMOW2 and VSLAP2 with average errors of  $\pm 0.05$  ‰ for  $\delta^{18}\text{O}$  and  $\pm 1.0$  ‰ for  $\delta^2\text{H}$ .  
316  
317  
318  
319  
320

### 321 198 **2.3 Calculations**

322 199  
323  
324 200 If the  $\delta^{18}\text{O}_{\text{calcite}}$  and water temperature at the time of calcite precipitation are known, the  
325 201 expected  $\delta^{18}\text{O}_{\text{water}}$  value can be calculated using one of several empirical equations. However,  
326 202 because ostracod shells do not calcify in oxygen-isotope equilibrium with their host water,  
327 203 corrections must be made for vital offsets. For *Cyprideis torosa*, the best estimate for the vital  
328 204 offset is  $\sim +0.8$  ‰ (Keatings *et al.*, 2007).  
329  
330  
331

332 206 The water temperature at the time of calcification can be determined using the Mg content for  
333 207 the corresponding valve to that used for isotope analysis, and the equation of De Deckker *et*  
334 208 *al.* (1999):  
335  
336  
337

$$338 \quad T(^{\circ}\text{C}) = 2.69 + (5230 * [\text{Mg}/\text{Ca}]_{\text{ostracod}} / [\text{Mg}/\text{Ca}]_{\text{water}}) \quad (1)$$

340 211  
341 212  
342 213 A  $\text{Mg}/\text{Ca}_{\text{water}}$  of 4.2 mol/mol (the average measured  $\text{Mg}/\text{Ca}_{\text{water}}$  value; Roberts *et al.*, 2020) is  
343 214 used in the equation.  
344  
345  
346

347 216 The Mg/Ca-inferred temperatures are combined with  $\delta^{18}\text{O}_{\text{ostracod}}$  values to determine  $\delta^{18}\text{O}_{\text{water}}$   
348 217 using Kim and O'Neil (1997):  
349  
350

$$351 \quad 1000 \ln \alpha_{(\text{calcite-water})} = 18.03(10^3 T^{-1}) - 32.42 \quad (2)$$

352 219  
353 220 Where  $T$  is in kelvins.  
354  
355  
356  
357  
358  
359  
360

361  
362  
363 223 The fractionation factor ( $\alpha_{\text{calcite-water}}$ ) can be calculated using:  
364  
365 224

$$\alpha_{\text{calcite-water}} = (1000 + \delta^{18}\text{O}_{\text{calcite}}) / (1000 + \delta^{18}\text{O}_{\text{water}}) \quad (3)$$

366 225  
367  
368 226  
369 227  
370  
371 228 Where both  $\delta^{18}\text{O}_{\text{calcite}}$  and  $\delta^{18}\text{O}_{\text{water}}$  are expressed relative to VSMOW. To convert from VPDB  
372 229 to VSMOW, the conversion proposed by Coplen *et al.* (1983) was used:  
373  
374 230

$$\delta^{18}\text{O}_{\text{VSMOW}} = 1.03091 * \delta^{18}\text{O}_{\text{VPDB}} + 30.91 \quad (4)$$

### 379 234 **3. Results**

#### 382 236 **3.1 Water isotope composition**

383  
384 237  
385 238  $\delta^{18}\text{O}_{\text{water}}$  values measured throughout the year ranged from  $-2.84$  to  $+4.85$  ‰. Highest  $\delta^{18}\text{O}$   
386  
387 239 values were recorded in August ( $+3.86$  ‰) and June ( $+4.85$  ‰) (Table 1; Fig. 2a). Water  
388 240 sampled in December to April had lower  $\delta^{18}\text{O}$  values, with the lowest value of  $-2.84$  ‰  
389  
390 241 recorded in December. There is a strong relationship ( $R^2 = 0.86$ ) between  $\delta^{18}\text{O}_{\text{water}}$  and  
391 242 electrical conductivity (EC) (Fig. 3): this relationship is particularly pronounced for the values  
392  
393 243 recorded in June when the highest  $\delta^{18}\text{O}_{\text{water}}$  values ( $+4.85$  ‰) and EC values ( $75.2$  mS  $\text{cm}^{-1}$ )  
394 244 are recorded (Fig. 2b). There is a strong distinction between the summer samples (June and  
395  
396 245 August) and samples taken in September to April; the summer months are characterised by  
397 246 high  $\delta^{18}\text{O}$  values. Water temperature and  $\delta^{18}\text{O}_{\text{water}}$  display similar trends with increasing values  
398  
399 247 between December 2016 and June 2017 (Fig. 2c) In September, the  $\delta^{18}\text{O}_{\text{water}}$  was close to the  
400 248 seawater equivalent ( $-0.06$  ‰ in the pond, and  $+0.27$  ‰ adjacent to Ramsgate Harbour) (Fig.  
401 249 4) and reflects a drop in EC (Fig. 2a,b). Spatially there is little variation in isotope composition  
402  
403 250 of pond water (Table 2);  $\delta^2\text{H}$  and  $\delta^{18}\text{O}$  were slightly lower at location 5 and 6 compared to the  
404  
405 251 southern end of the pond.

#### 406 252 407 253 **3.2 Ostracod shell chemistry**

408  
409 254  
410  
411 255  $\delta^{18}\text{O}_{\text{ostracod}}$  values also suggest a seasonal pattern; valves collected in April, June and  
412  
413 256 September 2017 have lower  $\delta^{18}\text{O}$  (with a mean value  $-6.10$  ‰) and those from December  
414 257 2016 and February 2017 are higher (a mean value of  $+1.80$  ‰) (Fig 2d; Table 3). All  $\delta^{18}\text{O}_{\text{ostracod}}$   
415  
416 258 values for April, June, and September 2017 are negative (minimum value of  $-11.38$  ‰), but

421  
422  
423 259 the mean  $\delta^{18}\text{O}_{\text{ostracod}}$  value for August 2016 is +1.24 ‰. For the August 2016, December 2016,  
424  
425 260 and February 2017 collections, the range of values is similar for all months ( $\pm 3.8$  ‰, 5.0 ‰,  
426  
427 261 and 4.3 ‰ respectively). For samples collected in April and September 2017 the range is  
428  
429 262 smaller at 2.6 and 2.9 ‰. The largest range is 7.2 ‰ for samples collected in June 2017.  
430  
431 263  $\text{Mg}/\text{Ca}_{\text{ostracod}}$  is also strongly seasonal with gradually decreasing values recorded in April to  
432  
433 264 September with the lowest average values in December and February (7.88 and 8.24  
434  
435 265 mmol/mol) (Fig. 2e; Table 3). The range of values is highest in August 2016 ( $\pm 22.09$  mmol/mol)  
436  
437 266 and June 2017 ( $\pm 22.45$  mmol/mol) (Fig. 2e).

436 267 If the seasonal variation in  $\delta^{18}\text{O}_{\text{ostracod}}$  were being controlled primarily by water temperature,  
437  
438 268 a negative relationship between  $\text{Mg}/\text{Ca}_{\text{ostracod}}$  and  $\delta^{18}\text{O}_{\text{ostracod}}$  would be expected. However,  
439  
440 269 such a relationship is not seen in this dataset as a whole, although there is a negative  
441  
442 270 relationship for the samples taken in August 2016, December 2016 and February 2017 (Fig.  
443  
444 271 5a). The majority of samples from April, June and September 2017 do not follow the  
445  
446 272 relationship defined by Kim and O'Neil (1997). There is also a distinct separation of the  
447  
448 273 relationship between  $\delta^{18}\text{O}_{\text{ostracod}}$  and  $\text{Sr}/\text{Ca}_{\text{ostracod}}$  for samples collected in April, June and  
449  
450 274 September 2017 from samples collected in August 2016, December 2016 and February 2017  
451  
452 275 (Fig. 5b); the former have  $\delta^{18}\text{O}_{\text{ostracod}}$  values equivalent to freshwater (mean of  $-6.14$  ‰) while  
453  
454 276 the latter are characterised by high  $\delta^{18}\text{O}_{\text{ostracod}}$  values (mean of  $+1.62$  ‰). Unlike  $\delta^{18}\text{O}_{\text{ostracod}}$   
455  
456 277 and  $\text{Mg}/\text{Ca}_{\text{ostracod}}$ ,  $\text{Sr}/\text{Ca}_{\text{ostracod}}$  is similar throughout the year ( $\pm 2.19$  mmol/mol) with the highest  
457  
458 278 value in June 2017 (4.23 mmol/mol) and lowest in August (2.04 mmol/mol) (Fig. 5b).

459  
460 279  
461  
462 280  $\delta^{13}\text{C}_{\text{ostracod}}$  values mirror those of  $\delta^{18}\text{O}_{\text{ostracod}}$ , with higher values in April 2017, June 2017, and  
463  
464 281 September 2017 when  $\delta^{18}\text{O}_{\text{ostracod}}$  values are lower (Fig. 2f). The  $\delta^{13}\text{C}$  values for August 2016  
465  
466 282 are unlike those observed for Summer in 2017; the average  $\delta^{13}\text{C}$  value for August 2016 is  $-$   
467  
468 283  $5.69$  ‰ compared with  $-0.59$  ‰ in June 2017 and  $+0.93$  ‰ in September 2017. The value of  
469  
470 284  $-5.69$  ‰ is similar to those recorded in December ( $-6.16$  ‰) and February 2016 ( $-6.16$  ‰)  
471  
472 285 when  $\delta^{18}\text{O}_{\text{ostracod}}$  values are higher. Furthermore, in April, June, and September 2017 there is  
473  
474 286 a positive relationship between  $\delta^{18}\text{O}_{\text{ostracod}}$  and  $\delta^{13}\text{C}_{\text{ostracod}}$  while the August 2016, December  
475  
476 287 2016, and February 2017 samples have a negative relationship (Fig. 5c). Whilst the samples  
477  
478 288 from April, June and September 2017 have a distinct separate clustering in terms of isotopic  
479  
480 289 composition, this is not reflected in the  $\text{Mg}/\text{Ca}$  and  $\text{Sr}/\text{Ca}$  values with no relationship seen  
481  
482 290 across the dataset (Fig. 5d).

### 471 291 472 292 **3.3 Back calculated $\delta^{18}\text{O}_{\text{water}}$** 473 293



481  
482  
483  
484  
485  
486  
487  
488  
489  
490  
491  
492  
493  
494  
495  
496  
497  
498  
499  
500  
501  
502  
503  
504  
505  
506  
507  
508  
509  
510  
511  
512  
513  
514  
515  
516  
517  
518  
519  
520  
521  
522  
523  
524  
525  
526  
527  
528  
529  
530  
531  
532  
533  
534  
535  
536  
537  
538  
539  
540

294 Back calculated  $\delta^{18}\text{O}_{\text{water}}$  values range from +5.37 to -7.65 ‰ (Table 3). For the two  
295 populations identified above (1 – individuals collected in August 2016, December 2016, and  
296 February 2017 and 2 – individuals collected in April, June, and September 2017), the back  
297 calculated values for August 2016, December 2016, and February 2017 are 5.37 to -1.86 ‰  
298 and 1.80 to -7.65 ‰ for April, June, and September 2017.

#### 300 4. Discussion

301  
302 In the pond at Pegwell Bay, the dominant controls on  $\delta^{18}\text{O}_{\text{ostracod}}$  are  $\delta^{18}\text{O}_{\text{water}}$  (influenced by  
303 input cycles of seawater and meteoric water) and temperature. Due to the shallow, well-mixed,  
304 and habitat homogeneity of the Pegwell Bay pond, it is reasonable to assume that the  
305 dominant control on  $\delta^{13}\text{C}_{\text{ostracod}}$  is the breakdown of organic matter in the near surface  
306 sediments from increasing terrestrial and aquatic productivity. For trace-element/ $\text{Ca}_{\text{ostracod}}$  the  
307 dominant controls in the Pegwell Bay pond are temperature for  $\text{Mg}/\text{Ca}_{\text{ostracod}}$  and  $\text{Sr}/\text{Ca}_{\text{water}}$  for  
308  $\text{Sr}/\text{Ca}_{\text{water}}$  (see Roberts *et al.*, 2020).

309  
310 In a biplot of water  $\delta^{18}\text{O}$  and  $\delta^2\text{H}$ , the values for Pegwell lie on a lower gradient to the global  
311 meteoric water line (GMWL) (Fig. 4), demonstrating evaporative loss along the local  
312 evaporative line (LEL), with the seawater end member falling close to the LEL. Seasonal  
313 samples further confirm that evaporation is predominately driving salinity in the pond with high  
314 EC and elevated  $\delta^{18}\text{O}$  values recorded in months with high water temperature and vice versa  
315 (August and December respectively; Table 1, Table 4). Evaporation therefore appears to be  
316 seasonal and to be particularly pronounced in the warmer months, with  $\delta^{18}\text{O}_{\text{water}}$  values  
317 reaching +4.85 ‰ in June 2017 (the pond also dried out in 2009; Google Maps Street View,  
318 2018). Samples from April with similar  $\delta^{18}\text{O}$  values to the seawater  $\delta^{18}\text{O}$  end member suggest  
319 that on occasion there was a direct input of seawater, which may occur at extreme tidal events  
320 such as the spring equinox tide. Furthermore, the  $\text{Mg}/\text{Ca}_{\text{water}}$  and  $\text{Sr}/\text{Ca}_{\text{water}}$  values of 4.14  
321 mol/mol and 0.010 mol/mol are similar to seawater, although  $\text{Mg}/\text{Ca}$  is slightly lower than that  
322 of average seawater (5.1 mol/mol) suggesting some dilution, while the  $\text{Sr}/\text{Ca}$  is slightly higher  
323 than that of average seawater (0.0089 mol/mol) (Chester, 2000). In summary, therefore,  
324 seawater input and evaporation appear to be a primary controls on  $\delta^{18}\text{O}_{\text{ostracod}}$  with summer  
325 samples reflecting high temperatures and high  $\delta^{18}\text{O}_{\text{water}}$  and autumn/winter samples to reflect  
326 lower temperatures, higher precipitation, and therefore lower  $\delta^{18}\text{O}_{\text{water}}$ .

327  
328 On PCA biplots of environmental variables for each collection,  $\delta^{18}\text{O}_{\text{water}}$  explains 79.28 % of  
329 the variance (Fig. 6). August, June, and September 2017 are characterised by higher  
330 temperature, with June and August also having higher EC and  $\delta^{18}\text{O}_{\text{water}}$ . Autumn/winter waters

541  
542  
543  
544  
545  
546  
547  
548  
549  
550  
551  
552  
553  
554  
555  
556  
557  
558  
559  
560  
561  
562  
563  
564  
565  
566  
567  
568  
569  
570  
571  
572  
573  
574  
575  
576  
577  
578  
579  
580  
581  
582  
583  
584  
585  
586  
587  
588  
589  
590  
591  
592  
593  
594  
595  
596  
597  
598  
599  
600

331 (i.e. October to November) are characterised by low temperature and low  $\delta^{18}\text{O}_{\text{water}}$ . However,  
332 the September  $\delta^{18}\text{O}_{\text{ostracod}}$  values show a discrete clustering (Fig. 5a) that may relate to the  
333 lower electrical conductivity and  $\delta^{18}\text{O}_{\text{water}}$  values in this month compared to others (Table 1).  
334 Furthermore, September back-calculated  $\delta^{18}\text{O}_{\text{water}}$  values are as low as  $-7.65\text{‰}$  (equivalent  
335 to the isotopic composition of rainfall for SE England: Darling et al., 2003), suggesting that  
336 valves calcified in waters with a much greater input of meteoric water. Using the Mg/Ca-  
337 inferred temperature and monitored water temperatures to track the calcification months of  
338 collected valves, the September 2017 collection reflects conditions between April and July  
339 2017. June and July 2017 received high rainfall (74.2 and 85.6 mm respectively compared  
340 with a mean of 42.7 and 47.6 mm between 1934 and 2016; Table 4). The monitored waters  
341 ( $-1.19\text{‰}$  for April 2017 and  $+4.85\text{‰}$  for June 2017), however, suggest a considerable degree  
342 of evaporative enrichment and/or significant seawater input, which is plausible given the high  
343 temperatures (Table 1) and our basic understanding of site systematics. If the monitored  
344  $\delta^{18}\text{O}_{\text{water}}$  values are considered when interpreting the dataset, it would appear that the pond is  
345 highly evaporated, however, it is clear that pond water was equivalent to groundwater or local  
346 precipitation during June and July. The composition of the pond can therefore shift quickly (on  
347 a less than monthly timescale).

348  
349 The  $\delta^{18}\text{O}_{\text{ostracod}}$  values show a complex relationship with temperature. The individual  $\delta^{18}\text{O}_{\text{ostracod}}$   
350 values for collection in August 2016, December 2016 and February 2017 show some scatter,  
351 but follow the relationship between water temperature and calcite oxygen-isotope values  
352 based on the equation of Kim and O'Neil (1997) (Fig. 5a). However,  $\delta^{18}\text{O}_{\text{ostracod}}$  values for  
353 collections in April, June and September 2017 do not follow this relationship, suggesting that  
354  $\delta^{18}\text{O}_{\text{water}}$  is a more important control on  $\delta^{18}\text{O}_{\text{ostracod}}$ . Despite this,  $\text{Mg}/\text{Ca}_{\text{ostracod}}$ ,  $\text{Sr}/\text{Ca}_{\text{ostracod}}$ ,  
355 temperatures and monitored  $\delta^{18}\text{O}_{\text{water}}$  values are not distinctly different than in August 2016,  
356 December 2016 and February 2017. The primary hydrological difference is that in July and  
357 August 2016 there was lower precipitation than the same period in 2017 (10.8 and 18.0 mm  
358 respectively; Met Office 2012), which is reflected in the back calculated  $\delta^{18}\text{O}_{\text{water}}$  values (mean  
359 values of  $+2.17\text{‰}$  for valves collected in August 2016 compared with  $-4.75\text{‰}$  for September  
360 2017), suggesting that  $\delta^{18}\text{O}_{\text{water}}$  becomes the primary control on  $\delta^{18}\text{O}_{\text{ostracod}}$  during periods of  
361 lower  $\delta^{18}\text{O}_{\text{water}}$ .

362  
363 Changes in  $\delta^{18}\text{O}$  and  $\delta^{13}\text{C}$  in individual shells and in the different sampling periods provides  
364 insight into the influences on carbon-isotope signatures at Pegwell. Shells with lower  $\delta^{18}\text{O}$   
365 have higher  $\delta^{13}\text{C}_{\text{ostracod}}$ , suggesting that a greater amount of freshwater in the pond  
366 accompanies an increase in aquatic productivity, assuming that  $\delta^{13}\text{C}_{\text{DIC}}$  is a first-order proxy  
367 for aquatic productivity. Shells with higher  $\delta^{18}\text{O}$  have lower  $\delta^{13}\text{C}_{\text{ostracod}}$ , suggesting that elevated

601  
602  
603 368 evaporation or input of seawater is accompanied by oxidation of terrestrially-derived organic  
604 369 matter. This shift in relationship of positive carbon-oxygen covariance at lower  $\delta^{18}\text{O}_{\text{water}}$  to  
605 370 negative at higher  $\delta^{18}\text{O}_{\text{water}}$  (Fig. 5c) suggests that above a certain  $\delta^{18}\text{O}_{\text{water}}$  threshold, aquatic  
606 371 productivity begins to decline. The interpretation of  $\delta^{13}\text{C}_{\text{ostracod}}$  in some coastal lakes, may  
607 372 therefore be dependent on understanding of the range of expected  $\delta^{18}\text{O}_{\text{water}}$ . Where there is a  
608 373 shift to a positive relationship between  $\delta^{18}\text{O}_{\text{ostracod}}$  and  $\delta^{13}\text{C}_{\text{ostracod}}$ , it reflects a major change in  
609 374 hydrological budget (Schwalb, 2003) for example precipitation to seawater as the primary  
610 375 hydrological input. If this relationship is therefore seen in palaeo-dataset, it may be used to  
611 376 identify changes in freshwater/seawater input to coastal lakes. Although generally accepted  
612 377 that coastal lagoons, lakes, and ponds have relatively little freshwater input (Oertel, 2005), it  
613 378 is possible that some coastal lakes may have very large variations in salinity and at times have  
614 379 very low salinity as a result of large inputs of meteoric water. In estuaries, increased freshwater  
615 380 inputs from increased river discharge are known to increase primarily productivity (Underwood  
616 381 and Kromkamp, 1999) due to increased nutrient loading. It is possible, therefore, that in  
617 382 Pegwell Bay increased precipitation is driving nutrient loading from surface run-off of the  
618 383 surrounding salt marsh, and thus increasing productivity. Conversely, during times of  
619 384 increased seawater input, tidal cycles and direct oceanic connection are increasing turbidity  
620 385 and thus decreasing aquatic productivity.

621 386  
622 387  $\delta^{18}\text{O}_{\text{water}}$  values in coastal lakes may therefore represent variations in inputs of meteoric water  
623 388 and seawater, suggesting that  $\delta^{18}\text{O}_{\text{ostracod}}$  is related to importance of inputs into the  
624 389 hydrological budget. Samples that show a relationship with temperature, as defined by Kim  
625 390 and O'Neil (1997), are those shells with higher  $\delta^{18}\text{O}$  while shells with lower  $\delta^{18}\text{O}$  do not follow  
626 391 a thermodynamic relationship (Fig. 5a), suggesting  $\delta^{18}\text{O}_{\text{water}}$ , and hydrological budget, as a  
627 392 more important control than temperature. If bulk multiple shells are analysed (i.e. many shells  
628 393 combined together as one sample) that contains individuals from multiple generations, which  
629 394 may not all relate to temperature, it is likely that temperatures cannot be accurately  
630 395 reconstructed. Where multiple single individuals are analysed, the spread of  $\text{Mg}/\text{Ca}_{\text{ostracod}}$   
631 396 values used alongside the range of  $\delta^{18}\text{O}_{\text{ostracod}}$  may aid in identifying where a temperature  
632 397 signal is present.

## 633 398 634 399 **5. Conclusions**

635 400  
636 401 The study highlights the importance of modern systematic studies, particularly in highly  
637 402 complex and variable environments such as coastal lakes. However, even with good  
638 403 understanding of modern environments, the interpretation of palaeo-stable isotope datasets  
639 404 for *C. torosa* is complex. In most circumstances,  $\delta^{18}\text{O}_{\text{water}}$  is a more dominant control on

661  
662  
663 405  $\delta^{18}\text{O}_{\text{ostracod}}$ , but with a dependence on temperature when there is a direct marine influence and  
664  
665 406 high  $\delta^{18}\text{O}_{\text{water}}$ . Since there is a shift in relationship between  $\delta^{18}\text{O}_{\text{ostracod}}$  and  $\delta^{13}\text{C}_{\text{ostracod}}$  between  
666 407 the populations that follow the water temperature/ $\delta^{18}\text{O}_{\text{ostracod}}$  relationship and those that do  
667  
668 408 not, if multiple individuals per stratigraphic level are analysed and the resulting  $\delta^{18}\text{O}_{\text{ostracod}}$  and  
669 409  $\delta^{13}\text{C}_{\text{ostracod}}$  data combined, it may be possible to determine if the direction of change indicates  
670  
671 410 a population that can be used as a proxy for temperature. It is clear, therefore, that simplistic  
672 411 interpretations of  $\delta^{18}\text{O}_{\text{ostracod}}$  data with or without modern data may be misleading. We  
673  
674 412 recommend that for future palaeoenvironmental research in marginal marine environments,  
675 413 stable isotope analyses should be: 1) undertaken on multiple single shells; and 2) where  
676 414 carapaces are preserved, paired with trace-element/Ca analyses on the same individual.  
677  
678 415

## 679 416 **Acknowledgements**

680  
681 417  
682 418 The research was funded by a studentship from the UK Natural Environment Research  
683  
684 419 Council as part of the London NERC DTP (NE/L002485/1). The authors thank Miles Irving for  
685 420 cartography assistance with Figure 1. We are grateful to John McAllister (Head of Reserves  
686  
687 421 (East), Kent Wildlife Trust) for permission to monitor water temperatures and collect samples  
688 422 in the Pegwell Bay pond.  
689  
690 423

## 691 424 **References**

- 692 425  
693 426 Anadón, P., F. Burjachs, M. Martín, J. Rodríguez-Lazaro, F. Robles, R. Utrilla & A. Vazquez, 2002.  
694 427 Paleoenvironmental evolution of the Pliocene Villarroya Lake, northern Spain. A  
695 428 multidisciplinary approach. *Sedimentary Geology* 148(1-2):9-27.  
696 429 Anadón, P., A. Moscariello, J. Rodríguez-Lazaro & M. L. Filippi, 2006. Holocene environmental  
697 430 changes of Lake Geneva (Lac Lemman) from stable isotopes ( $\delta^{13}\text{C}$ ,  $\delta^{18}\text{O}$ ) and  
698 431 trace element records of ostracod and gastropod carbonates. *Journal of Paleolimnology*  
699 432 35(3):593-616.  
700 433 Bodergat, A. M., C. Lecuyer, F. Martineau, A. Nazik, K. Gurbuz & S. Legendre, 2014. Oxygen  
701 434 isotope variability in calcite shells of the ostracod *Cyprideis torosa* in Akyatan Lagoon,  
702 435 Turkey. *Journal of Paleolimnology* 52(1-2):43-59.  
703 436 Bridgwater, N. D., T. H. E. Heaton & S. L. O'Hara, 1999. A late Holocene palaeolimnological record  
704 437 from central Mexico, based on faunal and stable-isotope analysis of ostracod shells. *Journal*  
705 438 *of Paleolimnology* 22(4):383-397.  
706 439 Carbonel, P., 1988. Ostracods and the transition between fresh and saline waters. In P. De  
707 440 Deckker, J.-P. Colin & J.-P. Peypouquet (Eds.) *Ostracoda in the earth sciences*: 157-173.  
708 441 Amsterdam: Elsevier.  
709 442 Chester, R., 2000. Marine geochemistry, 1 edn. John Wiley & Sons.  
710 443 Chivas, A. R., P. De Deckker, S. X. Wang & J. A. Cali, 2002. Oxygen-isotope systematics of the  
711 444 nektic ostracod *Australocypris robusta*. In Holmes, J. A. & A. R. Chivas (Eds) *The*  
712 445 *Ostracoda: Applications in Quaternary Research*. American Geophysical Union, Geophysical  
713 446 Monograph, 13: 301-313. Washington D.C.: AGU.  
714 447 Coplen, T. B., C. Kendall & J. Hopple, 1983. Comparison of Stable Isotope Reference Samples.  
715 448 *Nature* 302(5905):236-238.

721  
722  
723  
724  
725  
726  
727  
728  
729  
730  
731  
732  
733  
734  
735  
736  
737  
738  
739  
740  
741  
742  
743  
744  
745  
746  
747  
748  
749  
750  
751  
752  
753  
754  
755  
756  
757  
758  
759  
760  
761  
762  
763  
764  
765  
766  
767  
768  
769  
770  
771  
772  
773  
774  
775  
776  
777  
778  
779  
780

449 Darling, W.G., Talbot, J.C., 2003. The O & H stable isotopic composition of fresh waters in the  
450 British Isles. 1. Rainfall. *Hydrology and Earth System Sciences* 7, 163-181.

451 De Deckker, P., A. R. Chivas & J. M. G. Shelley, 1999. Uptake of Mg and Sr in the euryhaline  
452 ostracod *Cyprideis* determined from in vitro experiments. *Palaeogeography,*  
453 *Palaeoclimatology, Palaeoecology* 148(1-3):105-116.

454 De Deckker, P. & A. Lord, 2017. *Cyprideis torosa*: a model organism for the Ostracoda? *Journal of*  
455 *Micropalaeontology* 36(1), 3-6

456 Decrouy, L., T. W. Vennemann & D. Ariztegui, 2011. Controls on ostracod valve geochemistry: Part  
457 2. Carbon and oxygen isotope compositions. *Geochimica Et Cosmochimica Acta*  
458 75(22):7380-7399.

459 Dettman, D. L., A. J. Smith, D. K. Rea, T. C. Moore & K. C. Lohmann, 1995. Glacial meltwater in  
460 Lake Huron inferred from single-valve analysis of oxygen isotopes in ostracodes. *Quaternary*  
461 *Research* 43:297-310.

462 Dix, G. R., R. T. Patterson & L. E. Park, 1999. Marine saline ponds as sedimentary archives of late  
463 Holocene climate and sea-level variation along a carbonate platform margin: Lee Stocking  
464 Island, Bahamas. *Palaeogeography, Palaeoclimatology, Palaeoecology* 150(3-4):223-246.

465 Google Maps Street View. 'Sandwich Road Street View' [Map], Google,  
466 <https://goo.gl/maps/LMVmosyEEqN2>; accessed 07-Apr-20.

467 Heaton, T. H. E., J. A. Holmes & N. D. Bridgwater, 1995. Carbon and oxygen isotope variations  
468 among lacustrine ostracods: Implications for palaeoclimatic studies. *Holocene* 5(4):428-434.

469 Heip, C., 1976. The life-cycle of *Cyprideis torosa* (Crustacea, Ostracoda). *Oecologia* 24(3):229-245.

470 Hodell, D. A., J. H. Curtis, G. A. Jones, A. Higuera-Gundy, M. Brenner, M. W. Binford & K. T. Dorsey,  
471 1991. Reconstruction of Caribbean climate change over the past 10,500 years. *Nature*  
472 352(6338):790-793.

473 Holmes, J. A., T. Atkinson, D. P. F. Darbyshire, D. J. Horne, J. Joordens, M. B. Roberts, K. J. Sinka  
474 & J. E. Whittaker, 2010. Middle Pleistocene climate and hydrological environment at the  
475 Boxgrove hominin site (West Sussex, UK) from ostracod records. *Quaternary Science*  
476 *Reviews* 29(13-14):1515-1527

477 Ingram, B. L., P. De Deckker, A. R. Chivas, M. E. Conrad & A. R. Byrne, 1998. Stable isotopes,  
478 Sr/Ca, and Mg/Ca in biogenic carbonates from Petaluma Marsh, northern California, USA.  
479 *Geochimica Et Cosmochimica Acta* 62(19-20):3229-3237.

480 Janz, H. & T. W. Vennemann, 2005. Isotopic composition (O, C, Sr, and Nd) and trace element  
481 ratios (Sr/Ca, Mg/Ca) of Miocene marine and brackish ostracods from North Alpine Foreland  
482 deposits (Germany and Austria) as indicators for palaeoclimate. *Palaeogeography,*  
483 *Palaeoclimatology, Palaeoecology* 225(1-4):216-247.

484 Keatings, K. W., T. H. E. Heaton & J. A. Holmes, 2002. Carbon and oxygen isotope fractionation in  
485 non-marine ostracods: Results from a 'natural culture' environment. *Geochimica Et*  
486 *Cosmochimica Acta* 66(10):1701-1711.

487 Keatings, K., I. Hawkes, J. Holmes, R. Flower, M. Leng, R. Abu-Zied & A. Lord, 2007. Evaluation of  
488 ostracod-based palaeoenvironmental reconstruction with instrumental data from the arid  
489 Faiyum Depression, Egypt. *Journal of Paleolimnology* 38(2):261-283.

490 Kim, S. T. & J. R. Oneil, 1997. Equilibrium and nonequilibrium oxygen isotope effects in synthetic  
491 carbonates. *Geochimica Et Cosmochimica Acta* 61(16):3461-3475.

492 Leng, M. J. & J. D. Marshall, 2004. Palaeoclimate interpretation of stable isotope data from lake  
493 sediment archives. *Quaternary Science Reviews* 23(7-8):811-831.

494 Li, X. & W. Liu, 2014. Water salinity and productivity recorded by ostracod assemblages and their  
495 carbon isotopes since the early Holocene at Lake Qinghai on the northeastern Qinghai–  
496 Tibet Plateau, China. *Palaeogeography, Palaeoclimatology, Palaeoecology* 407:25-33.

497 Marco-Barba, J., E. Ito, E. Carbonell & F. Mesquita-Joanes, 2012. Empirical calibration of shell  
498 chemistry of *Cyprideis torosa* (Jones, 1850) (Crustacea: Ostracoda). *Geochimica Et*  
499 *Cosmochimica Acta* 93:143-163.

500 Met Office (2012): Met Office Integrated Data Archive System (MIDAS) Land and Marine Surface  
501 Stations Data (1853-current). NCAS British Atmospheric Data  
502 Centre, 2017. <http://catalogue.ceda.ac.uk/uuid/220a65615218d5c9cc9e4785a3234bd0>

781  
782  
783  
784  
785  
786  
787  
788  
789  
790  
791  
792  
793  
794  
795  
796  
797  
798  
799  
800  
801  
802  
803  
804  
805  
806  
807  
808  
809  
810  
811  
812  
813  
814  
815  
816  
817  
818  
819  
820  
821  
822  
823  
824  
825  
826  
827  
828  
829  
830  
831  
832  
833  
834  
835  
836  
837  
838  
839  
840

Oertel, G. F., 2005. Coastal Lakes and Lagoons. In Schwartz, M. L. (ed) *Encyclopedia of Coastal Science*. Springer Netherlands, Dordrecht, 263-266.

Pint, A. & P. Frenzel, 2017. Ostracod fauna associated with *Cyprideis torosa* - An overview. *Journal of Micropalaeontology* 36(1):113-119.

Roberts, L. R., J. A. Holmes & D. J. Horne, 2020. Tracking the seasonal calcification of *Cyprideis torosa* (Crustacea, Ostracoda) using Mg/Ca-inferred temperatures, and its implications for palaeotemperature reconstruction. *Marine Micropaleontology* 156:101838.

Romanek, C. S., E. L. Grossman & J. W. Morse, 1992. Carbon Isotopic Fractionation in Synthetic Aragonite and Calcite - Effects of Temperature and Precipitation Rate. *Geochimica Et Cosmochimica Acta* 56(1):419-430.

Scharf, B., M. Herzog & A. Pint, 2017. New occurrences of *Cyprideis torosa* (Crustacea, Ostracoda) in Germany. *Journal of Micropalaeontology* 36(1):120-126

Schwalb, A., 2003. Lacustrine ostracodes as stable isotope recorders of late-glacial and Holocene environmental dynamics and climate. *Journal of Paleolimnology* 29(3):267-351.

Street-Perrott, F. A., J. A. Holmes, M. P. Waller, M. J. Allen, N. G. H. Barber, P. A. Fothergill, D. D. Harkness, M. Ivanovich, D. Kroon & R. A. Perrott, 2000. Drought and dust deposition in the West African Sahel: A 5500-year record from Kajemarum Oasis, northeastern Nigeria. *Holocene* 10(3):293-302.

Underwood, G. J. C. & J. Kromkamp, 1999. Primary Production by Phytoplankton and Microphytobenthos in Estuaries. In Nedwell, D. B. & D. G. Raffaelli (Eds) *Advances in Ecological Research*. 29: 93-153. Amsterdam: Academic Press.

von Grafenstein, U., 2002. Oxygen-isotope studies of ostracods from deep lakes. In Holmes, J. A. & A. R. Chivas (Eds) *The Ostracoda: Applications in Quaternary Research*. American Geophysical Union, Geophysical Monograph, 13: 249-266. Washington D.C.: AGU.

von Grafenstein, U., H. Erlenkeuser & P. Trimborn, 1999a. Oxygen and carbon isotopes in modern fresh-water ostracod valves: assessing vital offsets and autecological effects of interest for palaeoclimate studies. *Palaeogeography, Palaeoclimatology, Palaeoecology* 148(1-3):133-152.

von Grafenstein, U., H. Erlenkeuser, A. Brauer, J. Jouzel & S. J. Johnsen, 1999b. A mid-European decadal isotope-climate record from 15,500 to 5000 years BP. *Science* 284(5420):1654-1657.

Wansard, G., 1996. Quantification of paleotemperature changes during isotopic stage 2 in the La Draga continental sequence (NE Spain) based on the Mg/Ca ratio of freshwater ostracods. *Quaternary Science Reviews* 15:237-245.

Williams, M., M. J. Leng, M. H. Stephenson, J. E. Andrews, I. P. Wilkinson, D. J. Siveter, D. J. Horne & J. M. Vannier, 2006. Evidence that Early Carboniferous ostracods colonised coastal flood plain brackish water environments. *Palaeogeography, Palaeoclimatology, Palaeoecology* 230(3-4):299-318.

Wouters, K., 2017. On the modern distribution of the euryhaline species *Cyprideis torosa* (Jones, 1850) (Crustacea, Ostracoda). *Journal of Micropalaeontology* 36(1):21-30

Wrozyna, C., Frenzel, P., Daut, G., Mäusbacher, R., Zhu, L., & Schwalb, A. (2012). Holocene lake-level changes of Lake Nam Co, Tibetan Plateau, deduced from ostracod assemblages and  $\delta^{18}\text{O}$  and  $\delta^{13}\text{C}$  signatures of their valves. In D.J. Horne, J. Holmes, J. Rodriguez-Lazaro & F.A. Viehberg (Eds.), *Ostracoda as proxies for Quaternary climate* (Vol. 17, pp. 281-295). Amsterdam: Elsevier

Xia, J., B. J. Haskell, D. R. Engstrom & E. Ito, 1997. Holocene climate reconstructions from tandem trace-element and stable-isotope composition of ostracodes from Coldwater Lake, North Dakota, USA. *Journal of Paleolimnology* 17(1):85-100.

## List of Figures

**Figure 1.** Location of the coastal pond at Pegwell Bay. The black triangle adjacent to Ramsgate harbour denotes the location of the seawater end member water sample taken on

841  
842  
843 555 18-Apr-2017. The inset map shows the location of samples taken on 27-Jun-2017. Samples  
844 556 were collected at 'X' for all sample dates and the triangle .

846 557  
847 558 **Figure 2.** a)  $\delta^{18}\text{O}_{\text{water}}$ , b) electrical conductivity, c) average water temperature, d)  $\delta^{18}\text{O}_{\text{ostracod}}$   
848 559 e)  $\text{Mg}/\text{Ca}_{\text{ostracod}}$ , and d)  $\delta^{13}\text{C}_{\text{ostracod}}$  for each sampling day. Data from individual valves are  
850 560 represented by the grey circles and the mean is denoted by the black line

852 561  
853 562 **Figure 3.** Relationship between  $\delta^{18}\text{O}_{\text{water}}$  and electrical conductivity over the sampling year.  
854 563 The triangle denotes the seawater end member sampled adjacent to Ramsgate Harbour on  
855 564 18-Apr-17.

857 565  
858 566 **Figure 4.**  $\delta^2\text{H}$  and  $\delta^{18}\text{O}$  values for water sampled in April and June from the coastal pond. The  
859 567 triangle denotes the seawater end member sampled adjacent to Ramsgate Harbour on 18-  
860 568 Apr-17. The solid black line denotes the Global Meteoric Water Line (GMWL). The dashed  
862 569 line denotes the local evaporation line (LEL) of  $y = 4.1x - 4.3$  ( $R^2$  0.97).

864 570  
865 571 **Figure 5.** Relationships between a)  $\delta^{18}\text{O}_{\text{ostracod}}$  and  $\text{Mg}/\text{Ca}$ -inferred temperature b)  $\delta^{18}\text{O}_{\text{ostracod}}$   
867 572 and  $\text{Sr}/\text{Ca}_{\text{ostracod}}$ , c)  $\delta^{18}\text{O}_{\text{ostracod}}$  and  $\delta^{13}\text{C}_{\text{ostracod}}$  and d)  $\text{Mg}/\text{Ca}_{\text{ostracod}}$  and  $\text{Sr}/\text{Ca}_{\text{ostracod}}$ . The purple  
868 573 line in (a) shows the relationship between water temperature and calcite oxygen-isotope  
869 574 value based on the equation of Kim and O'Neil (1997)

871 575  
872 576  
873 576 **Figure 6.** PCA biplots of environmental variables for each sampling day

## 874 577 875 578 **List of Tables**

876 579  
877 580 **Table 1.** Electrical conductivity, average water temperature,  $\delta^{18}\text{O}$ , and  $\delta^2\text{H}$  for each of the  
878 581 sampling days. Temperature is the average recorded over a 24-hour period, except for 4-Aug-  
880 582 18, which is averaged from data logger deployment at 14:40.

882 583  
883 584 **Table 2.** Water chemistry variables recorded from high to low tide on 27-Jun-17. Numbers  
884 585 appearing after the 12:00 sampling times (1,2 etc.) relate to the locations in Figure 1.

886 586  
887 587 **Table 3.** Ostracod  $\text{Mg}/\text{Ca}$ ,  $\delta^{18}\text{O}$  and  $\delta^{13}\text{C}$  for individual carapaces collected on each  
888 588 sampling day. The trace element/ $\text{Ca}$  and isotope analyses are from the same carapace.

890 589  
891 590 **Table 4.** Minimum, maximum and average monthly air and water temperature, and monthly  
892 591 rainfall for the monitoring period August 2016 to September 2017. Air temperature and  
893 592 precipitation data were downloaded from Met Office (2012)

593 **Table 1.** Electrical conductivity, average water temperature,  $\delta^{18}\text{O}$ , and  $\delta^2\text{OH}$  for each of the  
 594 sampling days. Temperature is the average recorded over a 24-hour period, except for 4-Aug-  
 595 18, which is averaged from data logger deployment at 14:40.

Date	Electrical conductivity (mS cm <sup>-1</sup> )	Salinity PSU	Average water temperature (°C)	$\delta^{18}\text{O}$ (‰ VSMOW)	$\delta^2\text{H}$ (‰ VSMOW)
04-Aug-16	55.2	36.6	20.9	+3.86	
01-Dec-16	40.2	25.7	3.0	-2.84	
02-Feb-17	45.1	29.2	8.3	-1.46	
18-Apr-17	44.6	28.8	10.2	-1.19	+1.3
27-Jun-17	75.2	~53*	17.2	+4.85	+15.48
28-Sep-17	33.3	20.8	18.3	-0.06	-6.3
Ramsgate				+0.27	+1.6

\*above scale for accurate conversion

600 **Table 2.** Water chemistry variables recorded from high to low tide on 27-Jun-17. Numbers  
 601 appearing after the 12:00 sampling times (1,2 etc.) relate to the locations in Figure 1.

Time / Location	$\delta^{18}\text{O}$ (‰)	$\delta^2\text{H}$ (‰)	Electrical conductivity (mS cm <sup>-1</sup> )	Water Temp. (°C)	Alkalinity as CaCO <sub>3</sub> equivalence (mg L <sup>-1</sup> )	
					CO <sub>3</sub> <sup>2-</sup>	HCO <sub>3</sub> <sup>-</sup>
<b>06:00</b>	+5.28	+16.7	70.5	15.8	0	266
<b>07:00</b>	+5.20	+16.8	75.0	16.4	0	266
<b>08:00</b>	+5.18	+16.2	75.9	17.6	0	244
<b>08:30</b>	+4.28	+10.6				
<b>09:00</b>	+5.14	+16.5	77.8	19.0	0	256
<b>10:00</b>	+5.11	+16.2	76.9	19.4	0	272
<b>12:00-1</b>	+5.17	+15.0	77.8	22.5	0	270
<b>12:00-2</b>	+4.92	+17.4	76.7	21.6		
<b>12:00-3</b>	+4.29	+16.2	72.3	21.5		
<b>12:00-4</b>	+4.06	+16.2	70.2	23.2		
<b>12:00-5</b>	+4.14	+12.9	71.7	21.9		
<b>12:00-6</b>	+4.24	+14.8	71.9	22.2		
<b>14:00</b>	+5.09	+16.3	77.9	23.3	0	260
<b>15:00</b>	+5.07	+17.8	78.2	24.7	14	254
<b>17:00</b>	+5.11	+17.3	78.8	22.6	0	248
<b>Average</b>	<b>+4.82</b>	<b>+15.4</b>	<b>75.2</b>	<b>20.8</b>		
<b>Std Dev.</b>	<b>±0.46</b>	<b>±2.03</b>	<b>±3.0</b>	<b>±2.7</b>		

607 **Table 3.** Ostracod Mg/Ca, Mg/Ca-inferred temperature,  $\delta^{18}\text{O}_{\text{shell}}$ , back-calculated  $\delta^{18}\text{O}_{\text{water}}$ ,  
 608 and  $\delta^{13}\text{C}_{\text{shell}}$  for individual carapaces collected on each sampling day. The trace element/Ca  
 609 and isotope analyses are from the same carapace.



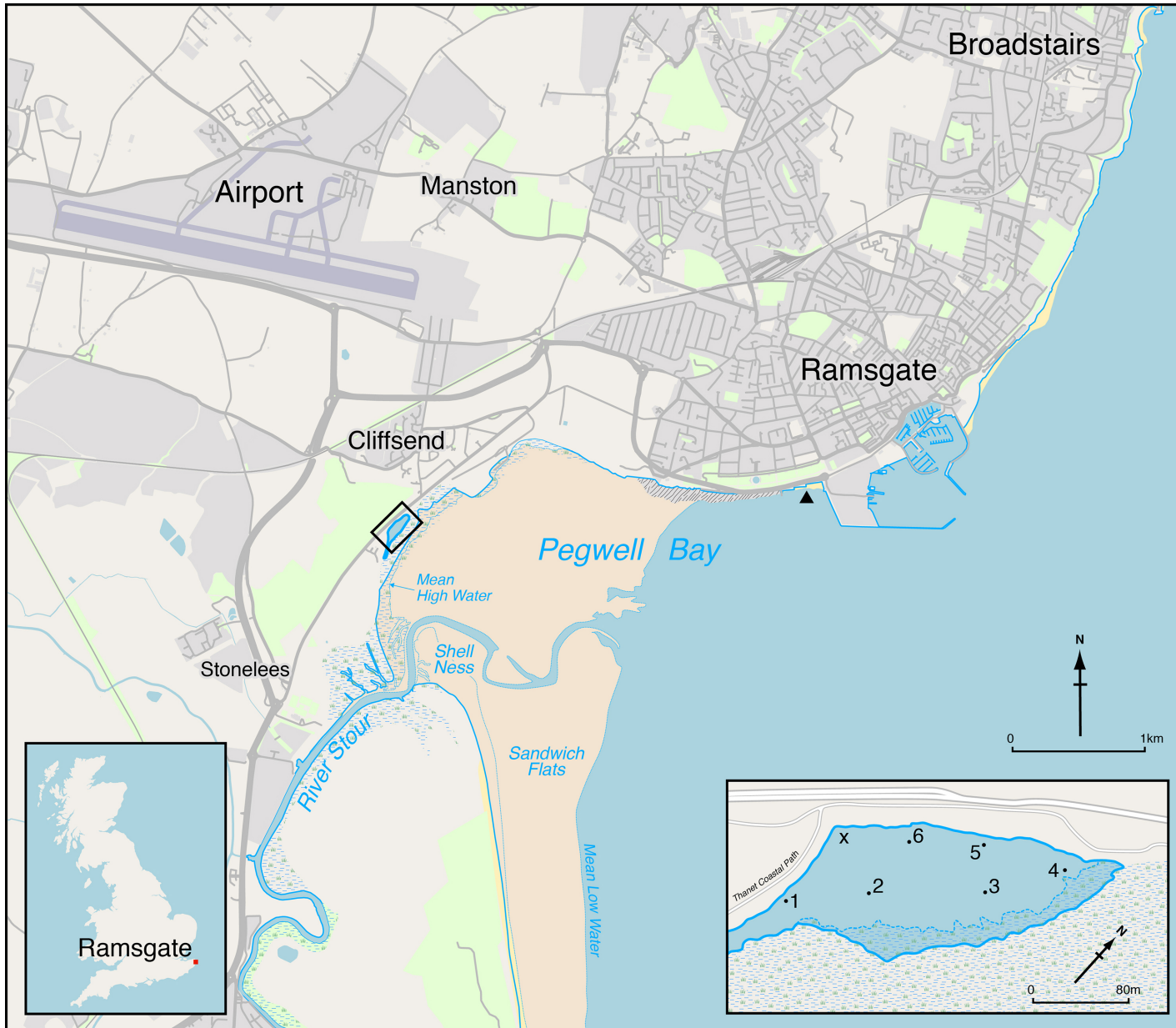
961  
962  
963  
964  
965  
966  
967  
968  
969  
970  
971  
972  
973  
974  
975  
976  
977  
978  
979  
980  
981  
982  
983  
984  
985  
986  
987  
988  
989  
990  
991  
992  
993  
994  
995  
996  
997  
998  
999  
1000  
1001  
1002  
1003  
1004  
1005  
1006  
1007  
1008  
1009  
1010  
1011  
1012  
1013  
1014  
1015  
1016  
1017  
1018  
1019  
1020

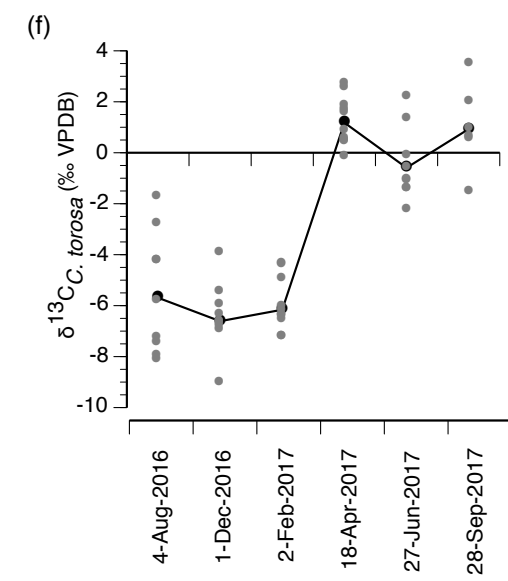
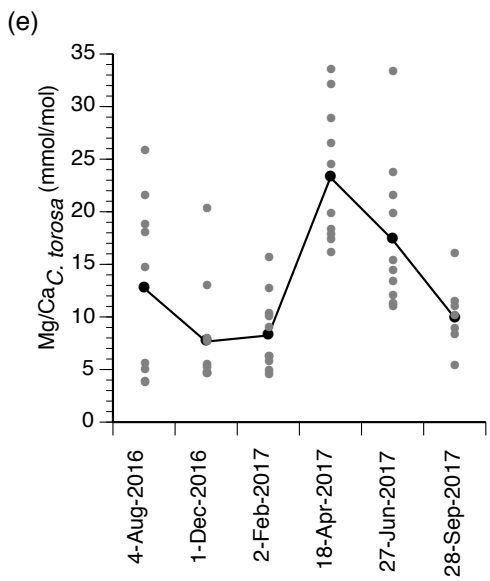
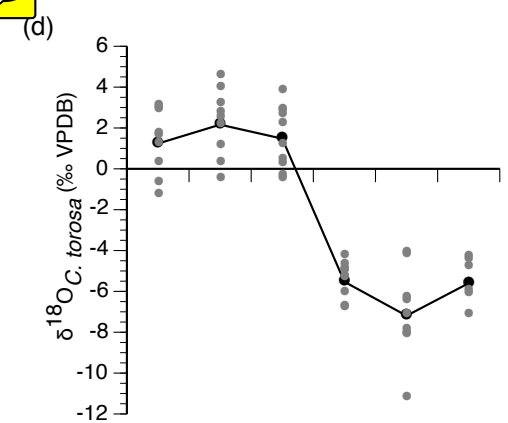
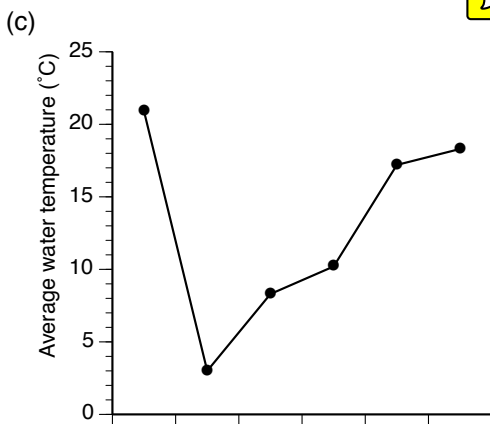
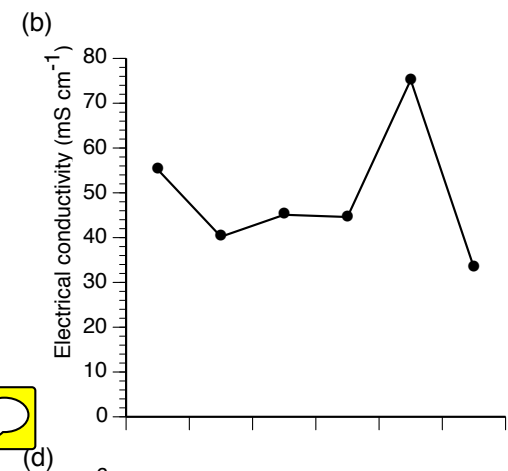
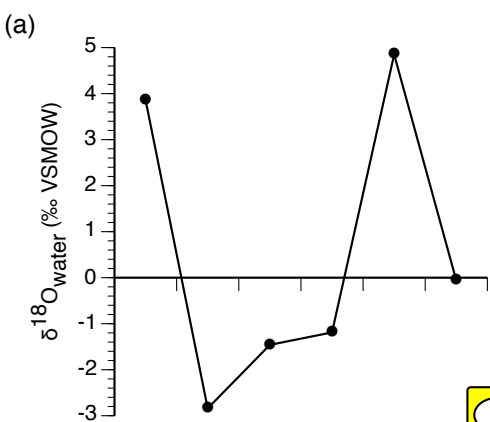
Collected	Mg/Ca <sub>ostracod</sub> (mmol/mol)	Mg/Ca- inferred Temperature (°C)	δ <sup>18</sup> O <sub>ostracod</sub> (‰)	Back- calculate d δ <sup>18</sup> O <sub>water</sub> (‰)	δ <sup>13</sup> C <sub>ostracod</sub> (‰)
	18.57	25.8	0.19	2.70	-2.91
	4.68	8.5	2.9	1.72	-7.67
	3.58	7.1	1.56	0.06	-8.35
	5.24	9.2	3.00	1.98	-7.45
<b>04-Aug-16</b>	17.78	24.8	1.65	3.96	-1.84
	14.39	20.6	-0.77	0.68	-6.01
	3.48	7	2.81	1.28	-8.20
	25.57	34.5	1.16	5.37	-4.41
	21.34	29.3	-1.37	1.83	-4.38
	12.75	18.6	2.08	3.11	-6.14
	4.93	8.8	2.44	1.33	-6.82
	7.64	12.2	3.12	2.77	-7.14
	4.35	8.1	4.49	3.22	-9.26
<b>01-Dec-16</b>	4.42	8.2	0.22	-1.03	-5.64
	7.33	11.8	2.69	2.25	-6.88
	4.27	8	-0.57	-1.86	-6.97
	20.05	27.7	1.07	3.95	-4.09
	5.19	9.2	3.92	2.90	-6.56
	4.57	8.4	-0.56	-1.76	-6.58
	4.24	8	-0.41	-1.71	-6.38
	5.48	9.5	0.16	-0.79	-5.13
	5.92	10.1	0.35	-0.47	-4.55
<b>02-Feb-17</b>	15.37	21.8	1.1	2.80	-4.52
	10.03	15.2	2.84	3.14	-7.41
	12.46	18.2	2.14	3.09	-6.58
	9.72	14.8	2.79	3.01	-6.25
	5.94	10.1	3.77	2.95	-6.76
	8.66	13.5	2.59	2.53	-7.42
	17.56	24.6	-5.45	-3.19	1.62
	18.03	25.1	-6.20	-3.83	-0.25
	28.67	38.4	-6.89	-1.95	2.64
	15.87	22.5	-5.10	-3.26	1.51
<b>18-Apr-17</b>	17.1	24	-5.41	-3.26	1.78
	24.24	32.9	-6.93	-3.03	2.48
	19.61	27.1	-5.08	-2.31	0.8
	33.32	44.2	-4.79	1.22	0.33
	31.91	42.4	-5.06	0.63	0.48
	26.26	35.4	-4.38	0.00	0.4

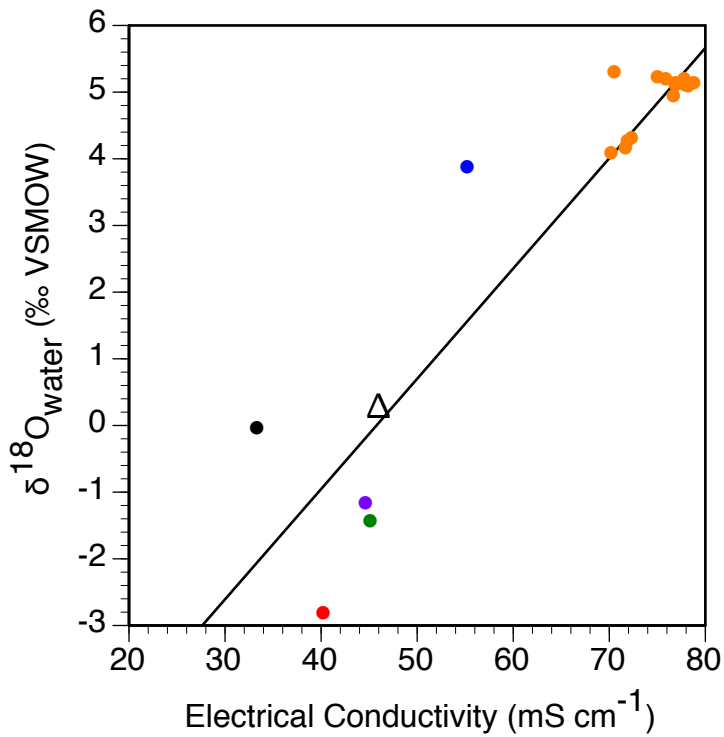
		13.06	19	-8.23	-7.12	-0.71
		33.12	43.9	-6.44	-0.49	-0.20
		21.34	29.3	-4.31	-1.10	2.14
		11.8	17.4	-4.21	-3.44	1.27
	<b>27-Jun-17</b>	23.5	32	-11.38	-7.65	-2.37
		15.11	21.5	-6.61	-4.97	-1.15
		11.01	27.1	-8.26	-5.49	-1.19
		14.18	16.4	-8.03	-7.47	-1.52
		10.67	20.3	-7.26	-5.88	-1.54
		9.89	16	-4.42	-3.95	0.87
		8.07	15	-4.93	-4.67	1.95
	<b>28-Sep-17</b>	5.08	12.7	-6.26	-6.50	0.45
		8.63	9	-4.59	-5.66	0.53
		11.22	13.4	-6.11	-6.20	3.44
		15.77	16.7	-7.28	-6.65	-1.66

**Table 4.** Minimum, maximum and average monthly air and water temperature, and monthly rainfall for the monitoring period August 2016 to September 2017. Air temperature and precipitation data were downloaded from Met Office (2012)

Month/Year	Air temp. (°C)			Water temp. (°C)			Precipitation (mm)
	Max.	Min.	Average	Max.	Min.	Average	
08/2016	23.3	14.4	18.5	27.4	13.0	19.4	18.0
09/2016	22.5	14.4	17.7	26.6	14.7	19.6	76.2
10/2016	15.0	9.4	11.9	17.1	9.8	12.8	34.8
11/2016	10.1	4.4	7.4	12.6	2.1	7.8	103.4
12/2016	9.3	3.8	6.8	10.1	0.4	5.7	9.2
01/2017	6.3	0.7	3.5	7.7	-1.6	3.3	48.2
02/2017	9.2	4.5	6.6	11.3	1.2	6.4	26.4
03/2017	13.0	6.0	9.2	16.4	4.7	10.2	17.2
04/2017	13.7	5.9	9.4	21.6	5.5	13.9	10.8
05/2017	17.9	9.9	13.5	31.0	8.1	17.6	57.8
06/2017	22.4	13.1	17.4	34.2	11.8	21.4	37.8
07/2017	22.8	14.5	18.0	30.9	13.9	20.6	74.2
08/2017	21.4	13.3	16.9	25.9	15.6	20.2	85.6
09/2017	18.3	11.1	14.3	22.9	12.3	16.8	37.0







● 4-Aug-2016

● 18-Apr-2017

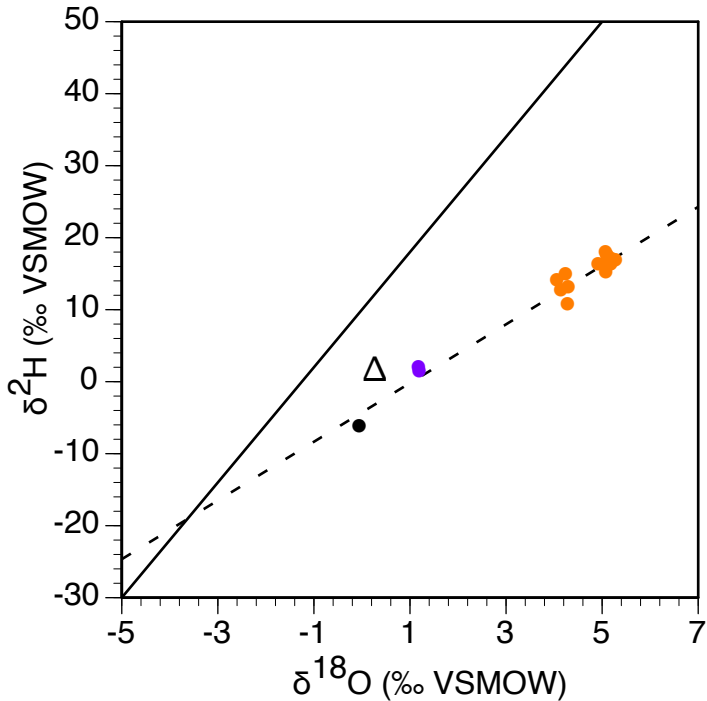
● 1-Dec-2016

● 27-Jun-2017

△ Ramsgate Harbour seawater

● 2-Feb-2017

● 28-Sep-2017



● 18-Apr-2017

● 28-Sep-2017

● 27-Jun-2017

△ Ramsgate Harbour seawater

